Electrical resistivity tomography revealing the internal structure of monogenetic volcanoes

Stéphanie Barde-Cabusson,[1] Xavier Bolós,[1] Dario Pedrazzi,[1] Raul Lovera,[2] Guillem Serra,[3] Joan Martí,[1] and Albert Casas[2]

Received 22 March 2013; revised 2 May 2013; accepted 6 May 2013.

[1] Eruptive activity of individual monogenetic volcanoes usually lasts a few days or weeks. However, their short lifetime does not always mean that their dynamics and structure are simple. Monogenetic cones construction is rarely witnessed from the beginning to the end, and conditions for observing their internal structure are hardly reached. We provide high-resolution electrical resistivity sections (10 m electrode spacing) of three monogenetic cones from northeastern Spain, comparing our results to geological observations to interpret their underground continuation. The 100 m maximum depth of exploration provides information on almost the entire edifices, highlighting the relationships between Strombolian and hydromagmatic deposits in two multiphase edifices. A main observation is a column of distinct resistivity centered on the Puig d'Adri volcano, which we interpret as the eruptive conduit. This method can provide valuable information on the past volcanic dynamics of monogenetic volcanic fields, which has real implications for the forecast of future activity.
Citation: Barde-Cabusson, S., X. Bolós, D. Pedrazzi, R. Lovera, G. Serra, J. Martí, and A. Casas (2013), Electrical resistivity tomography revealing the internal structure of monogenetic volcanoes, *Geophys. Res. Lett.*, *40*, doi:10.1002/grl.50538.

1. Introduction

[2] Monogenetic volcanoes are small volcanic edifices built-up in a short period of time, (e.g., few hours or days in the East-Izu monogenetic volcano group and several years for Jorullo in 1759 ~ 1766 and Paricutín in 1943 ~ 1952), so that their complexity is sometimes underestimated [*De la Cruz-Reyna and Yokoyama*, 2011]. Monogenetic volcanic edifices go from simple one-phase volcanoes to complex edifices built from several distinct phases of activity [*Walker*, 2000; *Valentine and Gregg*, 2008]. A complex eruptive dynamics can, for example, result in the accumulation of highly vesicular scoria (Strombolian-style explosive events) and compact, fine-enriched ash (phreatomagmatic explosive events), forming a complex layercake-style edifice alternating horizons of different electric resistivity material in a reduced space. This makes high-resolution electrical resistivity tomography (ERT) a valuable tool to investigate the internal structure of monogenetic volcanoes. In contrast with polygenetic volcanoes and despite being the most common type of activity, eruptions giving birth to monogenetic volcanoes are much less witnessed and less described in scientific reports [*Kereszturi and Németh*, 2012]. Only a few events of this type have occurred worldwide in historical times such as Al Madinah (1256), Jorullo (1759 ~ 1766) and Paricutín (1943 ~ 1952), and the Ukinrek maar (1977) [*De la Cruz-Reyna and Yokoyama*, 2011; *Kereszturi and Németh*, 2012]. Monogenetic cones can be weathered, exhibiting part of their internal structure. *Mathieu et al*. [2008] presented natural examples of monogenetic cones from the Chaîne des Puys (French Massif Central) and of parasitic cones from the northeast rift of Teide (Canary Islands) where the shape of shallow volcanic intrusions are well-preserved. Other examples exist [e.g., *Geshi et al*., 2011]; however, no unified model or similar attempted to connect field observations of this type with some geophysical approach until now.

[3] *Valentine* [2012] used crustal xenoliths to study the shallow plumbing systems of small-volume scoria cones and maars. In particular, he showed that their conduits or dikes flare mainly in the uppermost ~150 m of the crust.

[4] Geophysics has been successfully used to model [*Cassidy et al*., 2007; *Mrlina et al*., 2009; *Blaikie et al*., 2012] or to image [e.g., *Gebhardt et al*., 2011; *Martín-Serrano et al*., 2009; *Bolós et al*., 2012] the subsurface structure of maar volcanoes. ERT was applied on polygenetic volcanoes, providing valuable information on their structure and hydrothermal systems [e.g., *Revil et al*., 2008, 2011]. *Portal et al*. [2013] also presented preliminary results on a model of monogenetic dome using joint interpretation of ERT, gravimetry, and muonic imagery models. However, a detailed study of the internal structure of monogenetic volcanoes remains poorly documented, particularly edifices built up after multiple phases of activity.

[5] The Catalan Volcanic Zone (CVZ), at the north of Spain (Figure 1a), is mostly unknown compared to the contemporaneous alkaline volcanism in other parts of western and central Europe (Cenozoic alkaline volcanism in the Rhenish massif and Rhinegraben of Germany, the Massif Central of France, and the western Pannonian Basin in Eastern Europe; e.g., *Downes* [2001]) but it offers an excellent opportunity for a detailed exploration of monogenetic volcanoes' internal structure. In this study, we present ERT models from three monogenetic volcanoes giving a detailed image of the entire edifices. Key observations are made from the two more complex edifices because they offer the most important diversity of deposits and structural features.

[1]Institute of Earth Sciences Jaume Almera, ICTJA-CSIC, Lluis Sole i Sabaris s/n, Barcelona, Spain.
[2]Economic and Environmental Geology and Hydrology Group, Department of Geochemistry, Petrology and Geological Prospecting, Faculty of Geology, University of Barcelona, Barcelona, Spain.
[3]Polytechnic University of Catalonia, Barcelona, Spain.

Corresponding author: S. Barde-Cabusson, Institute of Earth Sciences Jaume Almera, ICTJA-CSIC, Lluis Sole i Sabaris s/n, 08028 Barcelona, Spain. (sbarde@ictja.csic.es)

©2013. American Geophysical Union. All Rights Reserved.
0094-8276/13/10.1002/grl.50538

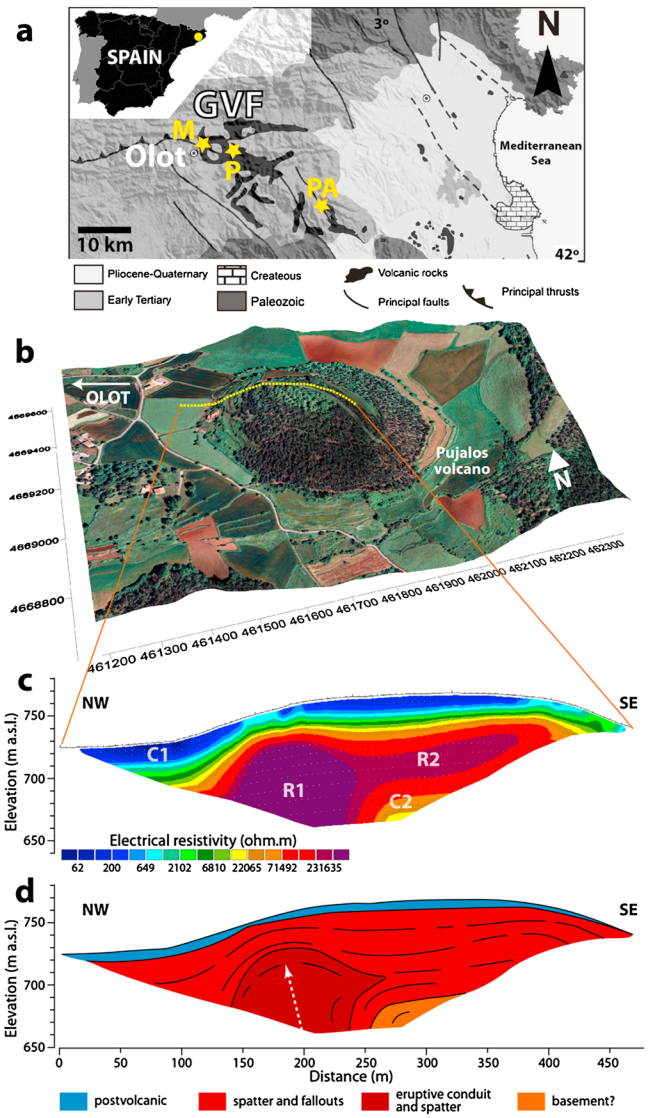

Figure 1. (a) Localization maps of the Garrotxa volcanic field (GVF) and of our three monogenetic volcanoes: Pujalós (P), Montsacopa (M), and Puig d'Adri (PA) volcanoes (modified from *Martí et al.* [2011]). (b) Orthophotography of the Pujalós volcano, a monogenetic Strombolian volcano, overlaid on a digital Elevation Model with localization of the ERT profile (yellow dotted line). (c) ERT model (RMS error 15.2% after five iterations). R and C stands for resistive and conductive bodies or layers respectively. (d) Geological interpretation.

2. Monogenetic Volcanism in the Garrotxa Volcanic Field

[6] The CVZ is one of the Quaternary alkaline volcanic provinces of the European rifts system [*Martí et al.*, 1992, 2011]. It has been active during the last 12 Ma and the volcanism is mainly characterized by alkali basalts and basanites. Inside the CVZ, the Garrotxa volcanic field is a subzone registering the latest volcanic activity (0.5–0.01 Ma) [*Araña et al.*, 1983; *Martí et al.*, 1992]. It comprises more than 50 well-preserved monogenetic volcanoes including scoria cones, tephra rings, and maars. Some of these eruptions alternated Strombolian and hydromagmatic phases, giving rise to complex stratigraphic successions not only within the monogenetic field but also at the scale of individual edifices [*Martí and Mallarach*, 1987; *Martí et al.*, 2011; *Pedrazzi and Marti*, 2011; *Bolós et al.*, 2012]. *Martí et al.* [2011] classify monogenetic volcanoes depending on whether or not hydromagmatic activity contributed to their construction. Volcanoes exclusively derived from magmatic activity correspond to scoria cones with occasional lava flows while volcanic cones including hydromagmatic activity, although morphologically similar to scoria cones, are much more complex. They may alternate phreatic, phreatomagmatic, and Strombolian phases, generating a wide diversity of pyroclastic density currents and fallout deposits, including explosive and effusive episodes.

3. Data Acquisition and Processing

[7] Multielectrode ERT was used to obtain 2-D resistivity high-resolution data on three monogenetic volcanoes from the Garrotxa volcanic field. We used an Iris Syscal Pro resistivity system with 48 electrodes connected to a 470 m long cable (10 m electrode spacing) in Wenner-Schlumberger configuration (maximum depth of investigation of about

100 m). We used the roll-along method to complete some of the profiles. No reciprocal measurements were taken but data quality was assessed by averaging or stacking several measurements and very good quality factors were obtained ($q < 3.5\%$). Low contact resistances of the electrodes were achieved because of the high moisture of the soils and the special design of the stainless steel electrodes directly in contact with the multicore cable (maximum values < 3 kΩ). Current injected was automatically adjusted by the system to optimize the input voltage and to ensure the best signal-to-noise ratio. The maximum power of the instrument is 800 V and the maximum current is 320 mA at 2.5 kΩ contact resistance. In our survey, depending on the distance between current electrodes, the current intensity ranged from 275 to 5 mA. The typical standard deviation was less than 1% with maximum standard deviation values lower than 3.5%.

[8] The resistivity data were inverted with RES2DINV [*Loke*, 2002]. Covariance matrix is commonly used to assess the accuracy of the inversion for models that consist of a small number of parameters but RES2DINV, like most nonlinear inversion programs, carries out an optimization process that tries to reduce the difference between the calculated and measured apparent resistivity values. The inversion routine used by the program is based on the smoothness-constrained least-squares method [*de Groot-Hedlin* and *Constable*, 1990; *Sasaki*, 1992] which allows to adjust the damping factor. This parameter is designed to accommodate noisier data sets, without which the inversion attempts to fit noise as data and becomes unstable. A larger damping factor was used for the Pujalós volcano data set (Figure 1). When data show large resistivity variations near the surface, it is also recommended to use a model where the cell width is half the unit electrode spacing. This was applied to the Pujalós and Montsacopa profiles. This strategy allowed us to improve the results but RMS error, estimating the difference between the calculated and measured apparent resistivity, was still high for Pujalós. The results are discussed taking this fact into account.

4. Results

[9] The following results relate to our three example monogenetic volcanoes. A first ERT profile was performed on the Pujalós volcano, near the city of Olot, in the Garrotxa volcanic field (Figure 1). The ERT cable was laid out from the northwestern side of the Pujalós, passing through the summit up to the southeastern flank (Figure 1b). The resistivity model (Figure 1c) shows a globally simple distribution of the resistivity. We found a superficial conductive layer C1 (<650 Ω·m), 10 to 20 m thick, and slightly thicker beyond the fields located at the NW of the cone. A rounded resistive body R1 (>250,000 Ω·m) appears at ~30 m depth. R1 is offset with respect to the cone summit and extends beyond the maximum depth of investigation. This resistive body seems to be connected to the SE with an elongated shape of slightly lower resistivity values that follows a 15° slope (R2). Under this layer, the resistivity values decrease progressively up to one order of magnitude (C2).

[10] The second test was performed in the same area, on Montsacopa, a volcano located inside the city of Olot itself. This volcano presents a NW-SE elongated shape with a well-preserved circular crater in the summit (crater B in Figure 2a). A previous study based on stratigraphy indicates the presence of a second eruptive vent (crater A in Figure 2a) on the SE flank [*Bolós*, 2009]. Our ERT profile (Figure 2b) covers the volcano nearly from one extreme to the other, crossing the two craters. This 710 m long profile is composed of two sections acquired with a roll-along of half the cable length. After four iterations, the data inversion gave a good RMS error value of 5.7%. The most striking feature is a 150 m wide high-resistivity body R3 (>200,000 Ω·m) under crater B. It presents a concave upper limit, nearly vertical laterals, and extends beyond the maximum depth of exploration. On top of this body lies a lenticular conductive body marked as C3, ~20 m thick at its maximum (~950 to 100 Ω·m). At the NW we observe a resistive elongated body (R4), dipping NW at an angle of 20°. It is surrounded by lower resistivity values (~3000 to 300 Ω·m). The resistivity distribution in the SE flank is more complex. It shows a few meters-thick superficial layer, displaying resistivity <3000 Ω·m. It overlays an irregular resistive layer with several tens of thousands Ω·m resistivity (R5). Surrounded by these high-resistivity values, the model shows a drop-shaped zone C4, of lower resistivity (~1000 Ω·m). Deeper, the inversion model shows resistivity values of about 3000 Ω·m.

[11] Still in the Garrotxa, we acquired a third ERT profile on the Puig d'Adri volcano (Figures 2d, 2e, 2f, and 1a for localization). These data were acquired along three sections overlapping by half the cable length, i.e., we obtained a profile of 950 m in total. After five iterations we obtained an RMS error of 6.1% for this model, confirming the quality of the inversion. The eastern part of the resistivity model shows several layers identified through their respective resistivity. In particular, we can notice the presence of a horizontal conductive layer (<400 Ω·m) at depth (C5). Going upward, an area of 1000 to 3000 Ω·m seems to change progressively from horizontal to ~20° dip. It lays under a more resistive (up to 8000 Ω·m) 20 m thick layer (R6). The rest of the resistivity model is occupied by a large resistive unit, R7, (>4000 Ω·m) overlaid by a conductive layer (<400 Ω·m). The resistive unit displays a V-shaped base, intersected by the lower limit of the model. Nearly in the center of the V, a less-resistive (light-red color in Figure 2e) vertical column connects the deepest layer to the surface. At 100 m to the west the conductive superficial layer enters deeper into the resistive unit. This last follows the slope of the western flank, forming a thick resistive layer (R8).

5. Discussion

[12] Our three example monogenetic volcanoes are a good illustration of the difference made by *Martí et al*. [2011] concerning monogenetic volcanoes affected or not by hydromagmatic phases during their construction. For the three sites, the water table is located in the sedimentary basement, at depths greater than our maximum depth of exploration so that we do not take it into account in the interpretation. Available geological information describes the Pujalós volcano as a scoria cone, possibly originating a lava flow covering an area of about 6 km^2 to the west [*IGC et al*., 2007]. Despite the elevated RMS error (15.2% after five iterations), the resistivity model seems to fit well this description (Figure 1). Moreover, a strong likeness exists with natural

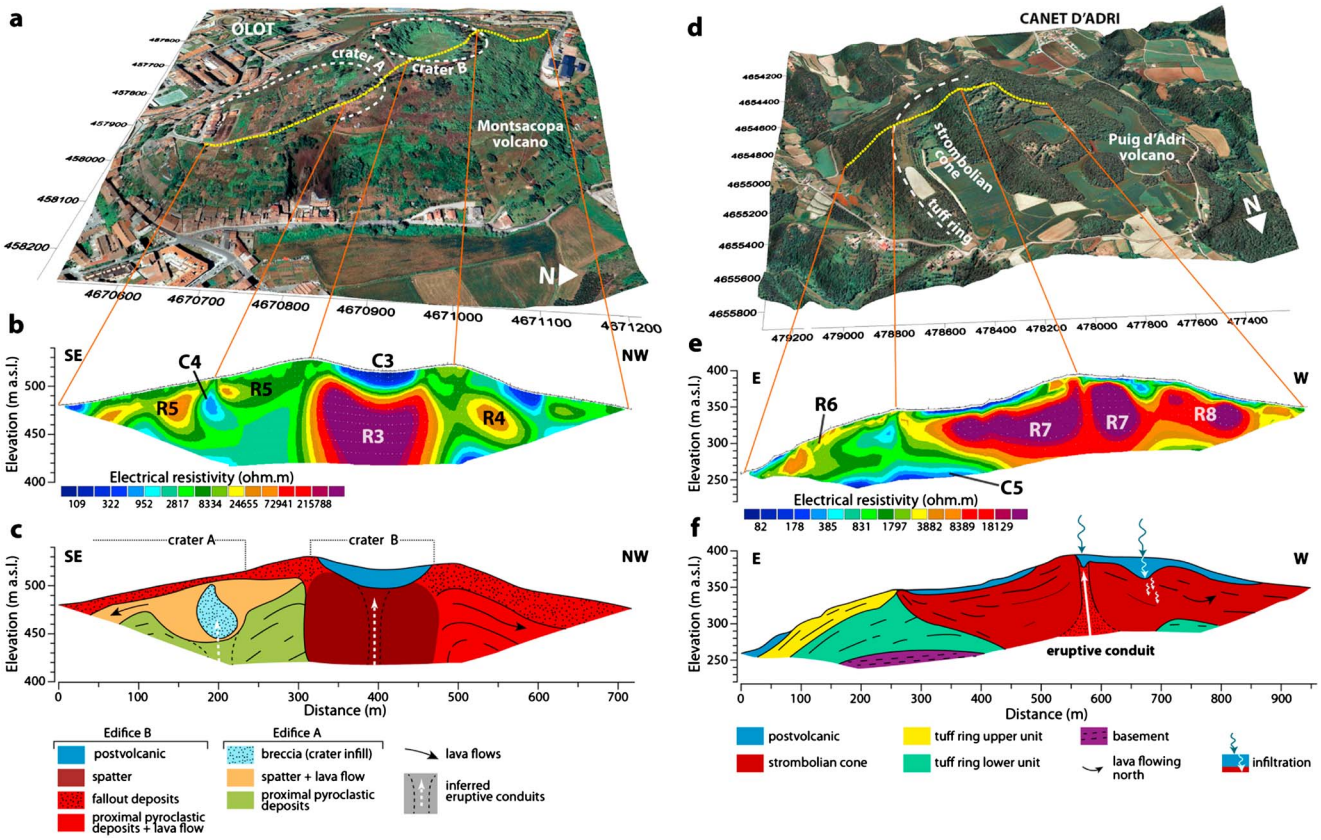

Figure 2. The Montsacopa and Puig d'Adri volcanoes, two complex monogenetic volcanoes built by hydromagmatic and Strombolian activity. (a and d) Orthophotography overlaid on a digital elevation model with localization of the ERT profile (yellow dotted line). (b and e) ERT model (vertical exaggeration 1.17, RMS error 5.7% after four iterations for Montsacopa and vertical exaggeration 1.17, RMS error 6.1% after five iterations for Puig d'Adri). R and C stands for resistive and conductive units respectively. (c and f) Geological interpretation.

examples from eroded areas such as the one we observed in El Hierro (Canary Islands, Spain). Figure 3 shows two buried monogenetic cones intersected by a vertical scarp on the coast of El Hierro. This situation allows observing a cross-section of both cones with their feeding dykes enlarging to flattened rounded massive units at the center of the volcanoes. This would correspond to the resistive heart R1 of the Pujalós volcano (Figure 1c). The conduit enlarging in the very superficial part of the eruptive system is quite compatible with conclusions made by *Valentine* [2012]. It can be interpreted as spatter deposits, which are the most proximal products to volcanic vents and directly connected to the eruptive conduit. In the Pujalós, resistive layer R2 can be compared to the stratified accumulation of scoria visible in the monogenetic cones of El Hierro. The resistivity values decreasing at depth (C2) may correspond to the basement, dipping NW. Because of the position of the profile we cannot confirm or infer the presence of a lava flow to the west. Finally, the conductive superficial layer C1 corresponds to the postvolcanic cover, thicker in the northwestern cultivated fields area.

[13] The repartition of the resistivity inside Montsacopa and Puig d'Adri appears more complex than for the Pujalós volcano, reflecting their more complex eruptive histories. Montsacopa shows a sequence involving a Strombolian phase at the beginning and a hydromagmatic one at the end [*Martí et al.*, 2011]. In addition to the summit well-visible crater, stratigraphical study of the volcanic deposits suggest the existence of a hidden vent on the southeastern flank [*Bolós*, 2009], which is confirmed by ERT. In the SE flank, we interpret the lower resistivity body C4 as crater A infill, i.e., breccias associated to Strombolian explosions (Figure 2b). This unit is likely surrounded by spatter deposits (R5). The connection with a feeding conduit is not visible on the tomogram, most probably because the profile is offset on a side of the crater. The continuation of R5 to the SE can be interpreted as a lava flow (Figure 2c). Under this system, the lower resistivity values may correspond to material with a higher open porosity and/or alteration [*Loke*, 2002]. According to the position of this unit in the edifice, it is compatible with fallout deposits that can be associated to the early activity of crater A. These deposits may have been cut-off to the NW by an explosion giving birth to crater B. This ~150 m wide cavity was likely filled by welded deposits forming R3 high-resistivity body. However, note that the inversion process may be affected by superficial strong resistivity contrasts [*Loke*, 2002] and the resistivity values of this body may be overestimated. These rocks being inaccessible and no similar rocks outcropping, no laboratory measurement of the real resistivity could be performed. The lenticular conductive layer C3 consists of postvolcanic products filling crater B. The NW flank of the volcano can be interpreted as an accumulation of proximal fallout deposits associated to crater B, with intercalation of more resistive lava flows (R4).

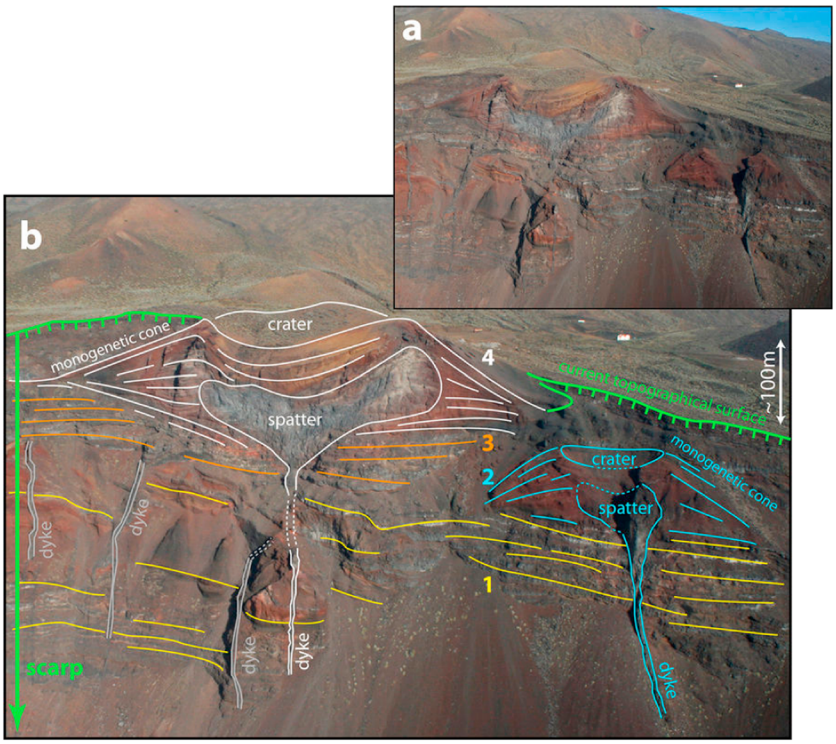

Figure 3. (a) Photography of two monogenetic cones intersected by a cliff at the western point of El Hierro (Canary Islands, Spain). (b) Interpretation. Numbers associated to a color code corresponds to a chronological order.

Indeed, outcrops at the NW of the volcano, close to our profile, show a superposition of two lava flows attributed to the activity of Montsacopa [*Bolós*, 2009].

[14] *Martí et al*. [2011] describe a complex eruptive history for the Puig d'Adri volcano, involving successive hydromagmatic and Strombolian phases. On the corresponding ERT profile the hydromagmatic deposits of the eastern side of the profile and the Strombolian deposits inside the limits of the tuff-cone [*Pujadas et al*., 1997; *Martí et al*., 2011] are well-identifiable (Figures 2e and 2f). In the east, the successive layers of different resistivity values correspond, from the surface to the base, to postvolcanic deposits on two hydromagmatic units. The upper hydromagmatic deposits (R6) show higher resistivity values with respect to the underlying deposits possibly because of a higher degree of compaction, reducing its permeability and then its water content. The underlying tuff ring deposits (Figure 2f) consist mainly of surges, explosion breccias, and a pyroclastic flow [*Martí et al*., 2011]. Conductive layer C5, visible at the inferior limit of the tomogram, likely corresponds to marls and sandstones constituting the basement. Its spatial relationship with both the hydromagmatic and Strombolian units and its resistivity, are fully compatible with this interpretation. The most uncommon observation provided by our ERT data concerns the Strombolian unit, represented in red tones in Figure 2f and corresponding to the highest resistivity values. A less-resistive 10 to 20 m large column occupies a central position inside the Strombolian cone and connects the deep layer to the surface. We believe that this lower resistivity values correspond to an accumulation of brecciated material partly consolidated, plugging the feeding conduit of the Strombolian cone. To our knowledge this is the first time that this has been shown with geophysical imaging. Finally, we interpret R8, at the western side of the profile, as the two lava flows described by *Martí et al*. [2011] that caused the breaching of the northwestern flank of the scoria cone. The underlying deposits are likely to be attributed to the hydromagmatic anterior phase. The interface between the lava flows and the Strombolian cone may constitute a preferential path for meteoric water infiltration, triggering progressive weathering of rocks and thus leading to decrease the resistivity. This would explain the deepening of the conductive superficial layer observed (blue arrow in Figure 2f). A similar explanation can be proposed for the slight deepening of the conductive superficial layer into the eruptive conduit, even if we are here at the limit of the spatial resolution of the ERT measurements.

6. Conclusion

[15] We show that volcanic cones exclusively derived from magmatic activity, built by the accumulation of scoria with occasional emission of lava flows, are easily distinguished from more complex edifices affected by hydromagmatic phases. ERT offers a strong advantage regarding spatial resolution and depth of exploration with respect to other geophysical methods, for the study of monogenetic volcanoes. With complementary surface geological observations either on site or using other natural examples, we could highlight various elements of the structure of these volcanoes and evidence several types of volcanic products such as (1) spatter deposits in the central part of the cones, (2) contrasts between hydromagmatic and Strombolian deposits, (3) buried lava flows, (4) the hidden eruptive vent of the Montsacopa volcano, and (5) the eruptive conduit of the Puig d'Adri Strombolian cone. We think that high-resolution ERT is a powerful tool for the study of the internal structure of monogenetic volcanoes. The detailed structural and geological

interpretation of such data is a valuable contribution to enhance knowledge about volcanic hazards in monogenetic volcanic fields in general. Because this method gives information about the past volcanic dynamics, it is particularly interesting for the forecast of future activity in a given monogenetic volcanic field.

[16] **Acknowledgments.** S. Barde-Cabusson was funded by JAE-Doc Program (JAEDoc_09_01319).This study was partially funded by the European Commission (FP7 Theme: ENV.2011.1.3.3-1; grant 282759: "VUELCO"), and by the grant *Beca d'investigació "Oriol de Bolós" en Ciències Naturals* (Olot, Spain). We thank the Natural Park of the Garrotxa Volcanic Zone for its support. We sincerely thank the Editor Andrew Newman, Karoly Nemeth and an anonymous reviewer for the improvements made from their comments.

[17] The Editor thanks Karoly Nemeth and an anonymous reviewer for their assistance in evaluating this paper.

References

Araña, V., A. Aparicio, C. Martín-Escorza, L. García Cacho, R. Ortiz, R. Vaquer, F. Barberi, G. Ferrara, J. Albert, and X. Gassiot (1983), El volcanismo Neógeno-Cuaternario de Catalunya: caracteres estructurales, petrológicos y geodinámicos, *Acta Geol. Hisp.*, *18*, 1–17.

Blaikie, T. N., L. Ailleres, R. A. F. Cas, and P. G. Betts (2012), Three-dimensional potential field modelling of a multi-vent maar-diatreme - The Lake Coragulac maar, Newer Volcanics Province, south-eastern Australia, *J. Volcanol. Geoth. Res.*, *235–236*, 70–83, doi:10.1016/j.jvolgeores.2012.05.002.

Bolós, X. (2009), Characterization of the Montsacopa volcano and its surroundings (in English, Spanish, and Catalan). Web access http://bit.ly/ZqkAaY, Garrotxa Volcanic Natural Parc, Olot, Spain.

Bolós, X., S. Barde-Cabusson, D. Pedrazzi, J. Martí, A. Casas, M. Himi, and R. Lovera (2012), Investigation of the inner structure of La Crosa de Sant Dalmai maar (Catalan Volcanic Zone, Spain), *J. Volcanol. Geoth. Res.*, *247–248*, 37–48, doi:10.1016/j.jvolgeores.2012.08.003.

Cassidy, J., S. J. France, and C. A. Locke (2007), Gravity and magnetic investigation of maar volcanoes, Auckland volcanic field, New Zealand, *J. Volcanol. Geoth. Res.*, *159*, 153–163, doi:10.1016/j.jvolgeores.2006.06.007.

De la Cruz-Reyna, S., and I. Yokoyama (2011), A geophysical characterization of monogenetic volcanism, *Geofis. Int.*, *50*(4), 465–484.

Downes, H. (2001), Formation and modification of the shallow subcontinental lithospheric mantle: a review of geochemical evidence from ultramafic xenolith suites and tectonically emplaced ultramafic massifs of Western and Central Europe, *J. Petrol.*, *42*, 233–250.

Gebhardt, A. C., M. De Batist, F. Niessen, F. S. Anselmetti, D. Ariztegui, T. Haberzettl, C. Kopsch, C. Ohlendorf, and B. Zolitschka (2011), Deciphering lake and maar geometries from seismic refraction and reflection surveys in Laguna Potrok Aike (southern Patagonia, Argentina), *J. Volcanol. Geoth. Res.*, *201*, 357–363, doi:10.1016/j.jvolgeores.2010.12.019.

Geshi, N., K. Németh, and T. Oikawa (2011), Growth of phreatomagmatic explosion craters: A model inferred from Suoana crater in Miyakejima Volcano, Japan, *J. Volcanol. Geoth. Res.*, *201*(1–4), 30–38, doi:10.1016/j.jvolgeores.2010.11.012.

de Groot-Hedlin, C., and S. Constable (1990), Occam's inversion to generate smooth, two-dimensional models from magnetotelluric data, *Geophysics*, *55*, 1613–1624.

Institut Geològic de Catalunya (IGC), Institut Cartogràfic de Catalunya (ICC), and Parc Natural de la Zona Volcànica de la Garrotxa (PNZVG) (2007), Carta Vulcanològica de la Zona Volcànica de la Garrotxa, 1:25.000, Ed.: Institut Cartografic de Catalunya, Barcelona.

Kereszturi G., and K. Németh (2012), Monogenetic Basaltic Volcanoes: Genetic Classification, Growth, Geomorphology and Degradation, in *Updates in Volcanology - New Advances in Understanding Volcanic Systems*, edited by K. Nemeth, Jeddah, Kingdom of Saudi Arabia, ISBN: 978-953-51-0915-0, InTech, doi:10.5772/51387.

Loke, M. H. (2002). RES2DINV ver. 3.54. Rapid 2-D resistivity and IP inversion using the least square method. Geotomo Software.

Martí, J., and J. M. Mallarach (1987), Erupciones hidromagmáticas en el volcanismo cuaternario de Olot, *Estudios Geológicos*, *43*, 31–40.

Martí, J., J. Mitjavila, E. Roca, and A. Aparicio (1992), Cenozoic magmatism of the Valencia trough (Western Mediterranean): relation between structural evolution and Volcanism, *Tectonophysics*, *203*, 145–166.

Martí, J., L. Planagumà, A. Geyer, E. Canal, and D. Pedrazzi (2011), Complex interaction between Strombolian and phreatomagmatic eruptions in the Quaternary monogenetic volcanism of the Catalan Volcanic Zone (NE of Spain), *J. Volcanol. Geoth. Res.*, *201*(1–4), 178–193.

Martín-Serrano, A., J. Vegas, A. García-Cortés, L. Galán, J. L. Gallardo-Millán, S. Martín-Alfageme, F. M. Rubio, P. I. Ibarra, A. Granda, A. Pérez-González, and J. L. García-Lobón (2009), Morphotectonic setting of maar lakes in the Campo de Calatrava Volcanic Field (Central Spain, SW Europe), *Sediment. Geol.*, *222*, 52–63.

Mathieu, L., B. van Wyk de Vries, E. P. Holohan, and V. R. Troll (2008), Dykes, cups, saucers and sills: Analogue experiments on magma intrusion into brittle rocks, *Earth Planet. Sci. Lett.*, *271*(1–4), 1–13, doi:10.1016/j.epsl.2008.02.020.

Mrlina, J., H. Kämpf, C. Kroner, J. Mingram, M. Stebich, A. Brauer, W. H. Geissler, J. Kallmeyer, H. Matthes, and M. Seidl (2009), Discovery of the first Quaternary maar in the Bohemian Massif, Central Europe, based on combined geophysical and geological surveys, *J. Volcanol. Geoth. Res.*, *182*, 97–112, doi:10.1016/j.jvolgeores.2009.01.027.

Pedrazzi, D., and J. Marti (2011), Interaction between Strombolian and phreatomagmatic eruptions in the monogenetic volcanic fields of the Iberian Peninsula and Lanzarote Island, A. Rittmann Conference, Nicolosi (Catania), 7–9 June 2011.

Portal, A., et al. (2013), Inner structure of the Puy de Dôme volcano: cross-comparison of geophysical models (ERT, gravimetry, muon imaging), *Geosci. Instrum. Method. Data Syst.*, *2*, 47–54, doi:10.5194/gi-2-47-2013.

Pujadas, A., L. Pallí, D. Brusi, and C. Roqué (1997), *El Vulcanisme de la Vall de Llémena*, Universitat de Girona, Spain (Eds.).

Revil, A., et al. (2008), Inner structure of La Fossa di Vulcano (Vulcano Island, southern Tyrrhenian Sea, Italy) revealed by high resolution electric resistivity tomography coupled with self-potential, temperature, and soil CO2 diffuse degassing measurements, *J. Geophys. Res.*, *113*, B07207, doi:10.1029/2007JB005394.

Revil, A., et al. (2011), Hydrogeology of Stromboli volcano, Aeolian Islands (Italy) from the interpretation of resistivity tomograms, self-potential, soil temperature, and soil CO2 concentration measurements, *Geophys. J. Int.*, *186*, 1078–1094, doi:10.1111/j.1365-246X.2011.05112.x.

Sasaki, Y. (1992), Resolution of resistivity tomography inferred from numerical simulation, *Geophys. Prospect.*, *40*, 453–464.

Valentine, G. A. (2012), Shallow plumbing systems for small-volume basaltic volcanoes, 2: Evidence from crustal xenoliths at scoria cones and maars, *J. Volcanol. Geoth. Res.*, *223–224*, 47–63, doi:10.1016/j.jvolgeores.2012.01.012.

Valentine, G. A., and T. K. P. Gregg (2008), Continental basaltic volcanism—processs and problems, *J. Volcanol. Geoth. Res.*, *177*, 857–873.

Walker, G. P. L. (2000), Basaltic volcanoes and volcanic systems, in *Encyclopedia of Volcanoes*, edited by Sigurdsson, H., pp. 283–289, Academic Press, San Francisco (CA).